

## Faddeev–type calculation of $\eta d$ threshold scattering

N. V. Shevchenko<sup>1,3</sup>, S. A. Rakityansky<sup>1,2</sup>, S. A. Sofianos<sup>2</sup>, V. B. Belyaev<sup>1,4</sup>  
and W. Sandhas<sup>5</sup>

- 1) *Joint Institute for Nuclear Research, Dubna, 141980, Russia*
- 2) *Physics Dept., University of South Africa, P.O.Box 392, Pretoria, South Africa*
- 3) *Physics Dept., Irkutsk State University, Irkutsk 664003, Russia*
- 4) *Research Center for Nuclear Physics, Osaka University, Mihogaoko 10–1, Ibaraki, Osaka 567, Japan*
- 5) *Physikalisches Institut, Universität Bonn, D-53115 Bonn, Germany*

### Abstract

The scattering length for the  $\eta$ -meson collision with deuteron is calculated on the basis of rigorous few-body equations (AGS) for various  $\eta N$  input. The results obtained strongly support the existence of a resonance or quasi-bound state close to the  $\eta d$  threshold.

PACS numbers: 25.80.-e, 21.45.+v, 25.10.+s

The production of  $\eta$  mesons and their collisions with nuclei have been studied experimentally and theoretically with increasing interest during the last years. To a large extent this is motivated by the fundamental questions of charge–symmetry breaking and the break–down of the Okubo–Zweig–Iizuka rule. Another relevant question concerns the possible formation of  $\eta$ –nucleus quasi–bound states.

In many respects the  $\eta$ -meson is similar to the  $\pi^0$ -meson despite it's being four times heavier. Both are neutral and spinless, they have almost the same lifetime,  $\sim 10^{-18}$  sec, and are the only mesons which have a high probability of pure radiative decay, that is, their quarks can annihilate into on-shell photons. However, when being involved in nuclear reactions they behave rather differently. The  $S_{11}$ -resonance  $N^*(1535)$ , for instance, is formed in both  $\pi N$  and  $\eta N$  systems, but at different collision energies,

$$E_{\pi N}^{res}(S_{11}) = 1535 \text{ MeV} - m_N - m_\pi \approx 458 \text{ MeV}$$

$$E_{\eta N}^{res}(S_{11}) = 1535 \text{ MeV} - m_N - m_\eta \approx 49 \text{ MeV}.$$

Thus, due to the large mass of the  $\eta$ -meson (547.45 MeV), this resonance is very close to the  $\eta N$ -threshold. Furthermore it is very broad, with  $\Gamma \approx 150$  MeV, covering the whole low energy  $\eta N$  region. As a result the interaction of nucleons with  $\eta$ -mesons in this region,

where the  $S$ -wave interaction dominates, is much stronger than with pions.

After its creation the  $N^*(1535)$ -resonance decays into  $\eta N$  and  $\pi N$  channels with equally high probabilities [1]

$$N^*(1535) \rightarrow \begin{cases} N + \eta & (35 - 55 \%) \\ N + \pi & (35 - 55 \%) \\ \text{other decays} & (\leq 10 \%) \end{cases}, \quad (1)$$

which indicates that the  $\eta N$  and  $\pi N$  interactions are to be treated by a coupled channel analysis. The resulting  $\eta N$  interaction, obtained in this way, turned out to be attractive [2]. This raises the question whether the attraction is strong enough to support  $\eta$ -nucleus quasi-bound states. Let us recall in this context that, because of their short lifetime,  $\eta$ -mesons can only be observed in final states of certain nuclear reactions. Within nuclei they are considered to undergo multiple absorption and production processes via the  $S_{11}$  resonance, with a final transition into pions. Such quasi-bound states therefore would be of considerable interest for studying  $\eta$ -meson properties in more detail.

For the calculation of these states various model treatments were employed, among them the optical potential method [3–6], the Green's function method [7], and the modified multiple scattering theory [8]. Calculations, based on the exact Alt–Grassberger–Sandhas (AGS) equations [9], for the  $\eta d$  system were also made in Ref. [10] in early nineties.

The predictions concerning the possibility of  $\eta$ -mesic nucleus formation are very diverse. One obvious reason for such a diversity is the poor knowledge of the  $\eta N$  forces. Another reason comes from the differences among the employed approximations some of which might be detrimental in view of the resonant character of the  $\eta N$  dynamics and the delicacy of the quasi-bound state problem. As was shown in Ref. [10] this problem cannot be adequately addressed by a meson–nucleus optical model or any low-order perturbation theory.

Among the approximate approaches the few-body dynamics of the  $\eta$ -nucleus systems was most explicitly treated in our previous calculations [11–15] based on the finite-rank approximation (FRA) of the nuclear Hamiltonians. The shortcoming of these calculations is the neglect of excitations of the nuclear ground states. This appears justified in the  $\eta^4\text{He}$  and possibly in the  $\eta$ -triton ( $^3\text{He}$ ) case, but is quite questionable in  $\eta$ -deuteron collisions.

In the present paper we, therefore, treat the  $\eta$ -deuteron system on the basis of the exact few-body equations (AGS). Both the  $NN$  and  $\eta N$  amplitudes entering them are chosen in separable form which reduces the dimension of these equations to one. The same  $\eta N$  amplitude have been used in the FRA calculations. This allows us to compare our present calculations of the  $\eta d$  scattering length with the previous approximate results, i.e., to examine the effect of the neglect of nuclear excitations employed in the FRA. It turns out that the discrepancies are not large for most of the  $\eta N$  parameter sets. This indicates that the conclusions drawn in our previous investigation [11–15] were already fairly reliable and should be even more reliable in the less sensitive  $\eta$ -triton or  $\eta^4\text{He}$  cases.

The  $\eta$ -deuteron scattering length is the value of the elastic scattering amplitude

$$f(\mathbf{p}'_1, \mathbf{p}_1; z) = -(2\pi)^2 \mu_1 \langle \mathbf{p}'_1; \psi_d | U_{11}(z) | \mathbf{p}_1; \psi_d \rangle \quad (2)$$

at zero collision energy. Here the subscript 1 labels the  $\eta(NN)$  partition and the  $\eta$ -deuteron channel whose asymptotic states are normalized as

$$\langle \mathbf{p}'_1; \psi_d | \mathbf{p}_1; \psi_d \rangle = \delta(\mathbf{p}'_1 - \mathbf{p}_1) .$$

The transition operator  $U_{11}$  obeys the system of AGS equations

$$U_{ij}(z) = (1 - \delta_{ij}) g_0^{-1}(z) + \sum_{k=1}^3 (1 - \delta_{ik}) t_k(z) g_0(z) U_{kj}(z) , \quad i, j = 1, 2, 3 , \quad (3)$$

where  $g_0$  is the free Green's function in the three-body space, and  $t_i$  the two-body  $T$ -matrix for the  $i$ -th pair ( $t_1 = t_{NN}$ ). For both  $t_{\eta N}$  and  $t_{NN}$  we used one-term separable forms

$$t_i(z) = |\chi_i\rangle \tau_i(z) \langle \chi_i| . \quad (4)$$

For the  $NN$  subsystem Eq. (4) implies that the asymptotic wave function is related to the form-factor  $|\chi_1\rangle$  according to

$$|\mathbf{p}_1; \psi_d\rangle = g_0(z) |\chi_1\rangle | \mathbf{p}_1 \rangle , \quad (5)$$

at  $z = p_1^2/2\mu_1 + E_d$  with  $E_d$  being the deuteron energy. Due to (4) and (5) the scattering amplitude (2) can be rewritten as

$$f(\mathbf{p}'_1, \mathbf{p}_1; z) = -(2\pi)^2 \mu_1 \langle \mathbf{p}'_1 | X_{11}(z) | \mathbf{p}_1 \rangle , \quad (6)$$

where the operators  $X_{ij}$ , defined as

$$X_{ij}(z) = \langle \chi_i | g_0(z) U_{ij}(z) g_0(z) | \chi_j \rangle ,$$

obey the system of equations

$$X_{ij}(z) = Z_{ij}(z) + \sum_{k=1}^3 Z_{ik}(z) \tau_k \left( z - \frac{p_k^2}{2\mu_k} \right) X_{kj}(z) \quad (7)$$

with

$$Z_{ij}(z) = (1 - \delta_{ij}) \langle \chi_i | g_0(z) | \chi_j \rangle .$$

The identity of the nucleons implies that  $X_{31} = X_{21}$ ,  $\tau_3 = \tau_2$ , and  $Z_{31} = Z_{21}$ , which reduces the system (7) to two coupled equations

$$\left\{ \begin{array}{l} X_{11}(z) = 2Z_{21}(z) \tau_2 \left( z - \frac{p_2^2}{2\mu_2} \right) X_{21}(z) , \\ X_{21}(z) = Z_{21}(z) + Z_{21}(z) \tau_1 \left( z - \frac{p_1^2}{2\mu_1} \right) X_{11}(z) + Z_{23}(z) \tau_2 \left( z - \frac{p_2^2}{2\mu_2} \right) X_{21}(z) . \end{array} \right. \quad (8)$$

Eventually, after making the  $S$ -wave projection of the matrix elements  $\langle \mathbf{p}'_i | X_{ij} | \mathbf{p}_j \rangle$  and  $\langle \mathbf{p}'_i | Z_{ij} | \mathbf{p}_j \rangle$ , we end up with one-dimensional integral equations which can be solved numerically by replacing the integrals by Gaussian sums.

The  $S$ -wave separable nucleon-nucleon and  $\eta$ -nucleon  $T$ -matrices of the form (4) were adopted from Refs. [16] and [11]. However the parameters originally proposed in Ref. [16] for the  $T$ -matrix

$$\begin{aligned} t_{NN}(p', p; z) &= \frac{1}{4\pi} v(p') \frac{A(z)}{1 - A(z)B(z)} v(p) , \\ v(p) &= \frac{\gamma}{\beta^2 + p^2} , \\ A(z) &= -\text{tgh} \left( 1 - \frac{z}{E_c} \right) , \\ B(z) &= \int_0^\infty \frac{p^2 v^2(p)}{z - p^2/m_N + i\varepsilon} dp , \end{aligned}$$

were slightly modified to  $E_c = 0.816 \text{ fm}^{-1}$ ,  $\beta = 1.604 \text{ fm}^{-1}$ , and  $\gamma^2 = 1.883 \text{ fm}^{-2}$  which correspond to more recent values of the triplet  $NN$  scattering length,  $a_{NN} = 5.424 \text{ fm}$ , and the effective range  $r_{NN} = 1.759 \text{ fm}$  [17,18]. With these parameters the deuteron is bound at 2.205 MeV and has an R.M.S.-radius  $\sqrt{\langle r^2 \rangle_d} = 1.887 \text{ fm}$ .

Instead of treating  $\eta N$  and  $\pi N$  as a two-channel system it is customary to describe the  $\eta N$  interaction by a one-channel complex potential. The strength parameter  $\lambda$  of the corresponding  $T$ -matrix,

$$t_{\eta N}(p', p; z) = \frac{\lambda}{(p'^2 + \alpha^2)(z - E_0 + i\Gamma/2)(p^2 + \alpha^2)} , \quad (9)$$

is chosen to reproduce the complex  $\eta$ -nucleon scattering length  $a_{\eta N}$ ,

$$\lambda = \frac{\alpha^4 (E_0 - i\Gamma/2)}{(2\pi)^2 \mu_{\eta N}} a_{\eta N} , \quad (10)$$

the imaginary part of which accounts for the flux losses into the  $\pi N$  channel. The range parameter  $\alpha$  in (9) is fixed in a somewhat more complicated way (see Refs. [2,20]), while  $E_0$  and  $\Gamma$  are the parameters of the  $S_{11}$  resonance [1],

$$E_0 = 1535 \text{ MeV} - (m_N + m_\eta) , \quad \Gamma = 150 \text{ MeV} .$$

The two-body scattering length  $a_{\eta N}$ , which defines the strength parameter  $\lambda$  via (10), is not accurately known. Different analyses [19] provided for  $a_{\eta N}$  the values in the range

$$0.27 \text{ fm} \leq \text{Re } a_{\eta N} \leq 0.98 \text{ fm} , \quad 0.19 \text{ fm} \leq \text{Im } a_{\eta N} \leq 0.37 \text{ fm} . \quad (11)$$

The parameter  $\alpha$  is also known with large uncertainty. Three different values are given in the literature, namely,  $\alpha = 2.357 \text{ fm}^{-1}$  [2],  $\alpha = 3.316 \text{ fm}^{-1}$  [20], and  $\alpha = 7.617 \text{ fm}^{-1}$  [2]. We, therefore, calculate the  $\eta$ -deuteron scattering length  $A_{\eta d}$  for values of  $a_{\eta N}$  and  $\alpha$  covering

these intervals. The results of our calculations are given in Tables 2, and 3, and also shown in Figs. 1 and 2.

In order to check our numerical procedure, we perform test calculation of the scattering length with decreasing values of the meson mass, and compare the results obtained with the corresponding scattering lengths given by

$$A_{\eta d}^{\text{FSA}} = -\frac{\mu}{\pi\alpha^4} \int_0^\infty \left\{ \frac{\mu}{\pi\alpha^4 r} \left[ r + \frac{e^{-\alpha r}}{2\alpha}(3 + \alpha r) - \frac{3}{2\alpha} \right] - \frac{1}{\lambda} \left( E_0 - \frac{i}{2}\Gamma \right) \right\}^{-1} |u_d(r)|^2 dr ,$$

where  $u_d$  is the radial wave function of the deuteron. This formula is easily derived in the Fixed Scatterer Approximation (FSA). As it should be, the AGS and FSA results converge to each other when the target particles become much heavier than the incident one (see Table 1.) .

In Table 2 we compare the present AGS calculations with our previous results obtained by means of the FRA [11]. In Table 3 we present  $A_{\eta d}$  calculated with  $\alpha = 3.316 \text{ fm}^{-1}$  for various values of  $a_{\eta N}$  given in the literature. For comparison, we show also the results of three different approximate calculations: that of Ref. [8] where two versions of the Multiple Scattering Theory (MST) were used, and a new FRA-calculations which we performed with the deuteron wave function (5). In contrast to our previous FRA calculations this wave function (which in the coordinate representation is of the Hulthen form) provides the same  $NN$  input as in the AGS calculations. The dependences of  $A_{\eta d}$  on  $\text{Re } a_{\eta N}$  and  $\text{Im } a_{\eta N}$  are shown in Fig. 1 and Fig. 2.

The curves depicted in Fig. 1 are similar to Argand plots, though they represent the scattering amplitude as a function of the coupling constant instead of the collision energy. Despite this the circular movement of the points on these curves is of the same nature as in the genuine Argand plot. Indeed, to draw an Argand plot one moves the point on the energy axis from left to right in the vicinity of a resonance pole. It is clear that if we fix the energy instead and move the resonance pole itself from right to left, the behavior of the amplitude should be similar to the Argand circle. An increase of  $\text{Re } a_{\eta N}$  makes the  $\eta N$  interaction more attractive which moves the  $\eta d$  resonance poles towards negative energies, i. e. from right to left. The Argand-like shape of the curves in Fig. 1 implies therefore that at a certain value of  $\text{Re } a_{\eta N}$  (within the interval from 0.25 fm to 1 fm) the resonance pole bypasses (from below) the point  $E = 0$  and becomes a quasi-bound pole.

It should be emphasized here that, in contrast to the genuine Argand plot, all the points depicted in Fig. 1 correspond to the same energy,  $E = 0$ , and therefore the range in which the  $\eta$ -deuteron  $S$ -matrix pole moves on the energy plane, when  $\text{Re } a_{\eta N}$  varies within its uncertainty interval, cannot be inferred from these circular curves. They, however, definitely indicate that such a pole exists and crosses the threshold line  $\text{Re } E = 0$ . The positions of this pole for different values of  $\text{Re } a_{\eta N}$  were explicitly calculated in a previous publication [15], where the FRA-approximation was employed. Recent measurements of  $\eta$  production in the reaction  $p + n \rightarrow d + \eta$  show a substantial enhancement of the cross section near threshold, as compared to what is expected from phase space analysis [26], implying the

existence of such a pole.

As can be seen in Table 3, both MST and FRA fail to give the correct  $A_{\eta d}$  (especially its real part) in the case of strong  $\eta N$  interaction (when  $\text{Re } a_{\eta N} > 0.5 \text{ fm}$ ) while for small values of  $\text{Re } a_{\eta N}$  these methods work reasonably well. Their failure in the case of strong two-body forces might be due to poor convergence of the multiple scattering series and to increased influence of the break-up channel.

To summarize, in the present work we perform exact AGS calculations for the  $\eta d$  scattering length for various  $\eta N$  input that include new data which appeared since the first calculation in 1991 [10]. The results obtained with these new data strongly suggest that a resonance or quasi-bound state could exist near the  $\eta d$  threshold, in agreement with the prediction of Ref. [10].

## ACKNOWLEDGMENTS

Financial support from the Russian Foundation for Basic Research, Deutsche Forschungsgemeinschaft, NATO (grant #CR-GLG970110), INTAS (grant #96-0457), and the Foundation for Research Development of South Africa is greatly appreciated.

## REFERENCES

- [1] Particle Data Group, Phys. Rev. D **50**(3), 1319 (1994).
- [2] R. S. Bhalerao, L. C. Liu, Phys. Rev. Lett. **54**, 865 (1985).
- [3] C. Wilkin, Phys. Rev. C **47**, R938 (1993).
- [4] C. Wilkin, Phys. Lett. B **331**, 276 (1994).
- [5] L. C. Liu, Q. Haider, Phys. Rev. C **34**, 1845 (1986).
- [6] H. C. Chiang, E. Oset, L. C. Liu, Phys. Rev. C **44**, 738 (1991).
- [7] G. L. Li, W. K. Cheng, T. T. S. Kuo, Phys. Lett. B **195**, 515 (1987).
- [8] A. M. Green, J. A. Niskanen, S. Wycech, Phys. Rev., C **54**, 1970 (1996).
- [9] E. O. Alt, P. Grassberger, and W. Sandhas, Nucl. Phys., B **2**, 167 (1967).
- [10] T. Ueda, Phys. Rev. Lett., **66**, 297 (1991).
- [11] S. A. Rakityansky, S. A. Sofianos, W. Sandhas, and V. B. Belyaev, Phys. Lett. B **359**, 33 (1995).
- [12] V. B. Belyaev, S. A. Rakityansky, S. A. Sofianos, W. Sandhas, and M. Braun, Few-Body Systems Suppl. **8**, 312 (1995).
- [13] S. A. Rakityansky, S. A. Sofianos, V. B. Belyaev, and W. Sandhas, Few-Body Systems Suppl., **9**, 227 (1995).
- [14] S. A. Rakityansky, V. B. Belyaev, S. A. Sofianos, M. Braun, W. Sandhas, Chinese J. Phys., **34**, 998 (1996).
- [15] S. A. Rakityansky, S. A. Sofianos, M. Braun, V. B. Belyaev, W. Sandhas, Phys. Rev., C **53**, R2043 (1996).
- [16] H. Garcilazo, Lett. Nuovo Cim., **28**, 73 (1980).
- [17] C. W. Wong, Nucl. Phys., A **536**, 269 (1992).
- [18] O. Dumbrajs et al., Nucl. Phys., B **216**, 277 (1983).
- [19] M. Batinic, I. Slaus, A. Svarc, Phys. Rev. C **52**, 2188 (1995).
- [20] C. Bennhold and H. Tanabe, Nucl. Phys., A **530**, 625 (1991).
- [21] B. Krusche, *Proceedings of II TAPS Workshop*, Guardamar, 1993, ed. by J. Diaz and Y. Schuts (World Scientific, Singapore,1994), p. 310.
- [22] M. Batinic, I. Slaus, A. Svarc, and B. M. K. Nefkens, Phys. Rev., C **51**, 2310 (1995).
- [23] Ch. Sauerman, B. L. Friman, and W. Nörenberg, Phys. Lett., B **341**, 261 (1995).
- [24] V. V. Abaev, B. M. K. Nefkens, Phys. Rev., C **53**, 385 (1996).
- [25] M. Arima, K. Shimizu, and K. Yazaki, Nucl. Phys., A **543**, 613 (1992).
- [26] H. Calén et al., Phys. Rev. Lett., **80**, 2069 (1998).

TABLES

TABLE I. Convergence of the AGS and FSA results for decreasing sequence of the meson mass values. The parameters of the  $\eta N$ -potential are fixed by  $a_{\eta N} = (0.75 + i0.27)$  fm and  $\alpha = 2.357 \text{ fm}^{-1}$ .

$\eta$ -mass	$A_{\eta d}^{\text{AGS}}$ (fm)	$A_{\eta d}^{\text{FSA}}$ (fm)
$m_\eta$	$3.941 + i6.702$	$1.936 + i3.162$
$m_\eta/2$	$1.548 + i0.596$	$1.374 + i0.856$
$m_\eta/3$	$0.891 + i0.283$	$0.878 + i0.439$
$m_\eta/4$	$0.629 + i0.185$	$0.640 + i0.292$
$m_\eta/5$	$0.487 + i0.138$	$0.503 + i0.218$
$m_\eta/10$	$0.230 + i0.061$	$0.242 + i0.095$
$m_\eta/20$	$0.113 + i0.029$	$0.119 + i0.045$
$m_\eta/30$	$0.075 + i0.019$	$0.079 + i0.029$
$m_\eta/40$	$0.056 + i0.014$	$0.059 + i0.022$
$m_\eta/50$	$0.045 + i0.011$	$0.047 + i0.017$

TABLE II. Comparison of  $\eta d$  scattering lengths (in fm), obtained using the AGS and FRA methods, for 9 combinations of the parameters of the  $\eta N$ -potential.

	$\alpha = 2.357 \text{ (fm}^{-1}\text{)}$	$\alpha = 3.316 \text{ (fm}^{-1}\text{)}$	$\alpha = 7.617 \text{ (fm}^{-1}\text{)}$	$a_{\eta N} \text{ (fm)}$
AGS	$0.71 + i0.79$	$0.71 + i0.84$	$0.71 + i0.92$	$0.27 + i0.22$
FRA	$0.66 + i0.82$	$0.65 + i0.85$	$0.62 + i0.89$	
AGS	$0.79 + i0.68$	$0.81 + i0.73$	$0.83 + i0.81$	$0.28 + i0.19$
FRA	$0.75 + i0.73$	$0.74 + i0.76$	$0.72 + i0.81$	
AGS	$1.81 + i2.44$	$1.64 + i2.99$	$0.75 + i4.00$	$0.55 + i0.30$
FRA	$1.53 + i2.00$	$1.38 + i2.15$	$1.14 + i2.22$	



TABLE III. Results of the AGS and three different approximate calculations of  $A_{\eta d}$  with  $\alpha = 3.316 \text{ fm}^{-1}$ .

$\eta N$ -input		exact $A_{\eta d}$ (fm)	approximate $A_{\eta d}$ (fm)		
Ref.	$a_{\eta N}$ (fm)	AGS	MST I [8]	MST II [8]	FRA
[20]	$0.25 + i0.16$	$0.73 + i0.56$	$0.66 + i0.71$	$0.66 + i0.58$	$0.65 + i0.70$
[2]	$0.27 + i0.22$	$0.71 + i0.84$	$0.57 + i0.97$	$0.64 + i0.81$	$0.59 + i0.96$
[21]	$0.291 + i0.360$	$0.38 + i1.36$	$0.17 + i1.35$	$0.42 + i1.25$	$0.21 + i1.35$
[3]	$0.30 + i0.30$	$0.61 + i1.22$	$0.39 + i1.28$	$0.58 + i1.11$	$0.42 + i1.27$
[21]	$0.430 + i0.394$	$0.50 + i2.07$	$0.14 + i1.91$	$0.65 + i1.73$	$0.24 + i1.88$
[2]	$0.44 + i0.30$	$1.15 + i1.89$	$0.63 + i1.93$	$1.01 + i1.50$	$0.68 + i1.86$
[20]	$0.46 + i0.29$	$1.31 + i1.99$	$0.72 + i2.04$	$1.11 + i1.54$	$0.76 + i1.96$
[22]	$0.476 + i0.279$	$1.49 + i2.06$	$0.81 + i2.15$	$1.22 + i1.56$	$0.84 + i2.05$
[23]	$0.51 + i0.21$	$2.37 + i1.77$	$1.48 + i2.31$	$1.65 + i1.39$	$1.38 + i2.22$
[3]	$0.55 + i0.30$	$1.64 + i2.99$	$0.61 + i2.73$	$1.40 + i1.98$	$0.69 + i2.51$
[21]	$0.579 + i0.399$	$0.34 + i3.31$	$-0.13 + i2.64$	$0.93 + i2.41$	$0.13 + i2.52$
[24]	$0.62 + i0.30$	$1.80 + i4.30$	$0.36 + i3.36$	$1.65 + i2.41$	$0.55 + i2.95$
[22]	$0.876 + i0.274$	$-8.81 + i4.30$	$-2.76 + i4.24$	$2.42 + i5.55$	$-0.67 + i3.98$
[22]	$0.888 + i0.274$	$-8.63 + i3.49$	$-2.90 + i4.12$	$2.37 + i5.79$	$-0.73 + i3.99$
[25]	$0.98 + i0.37$	$-4.69 + i1.59$	$-2.75 + i2.77$	$-0.06 + i6.20$	$-1.18 + i3.59$

FIGURES

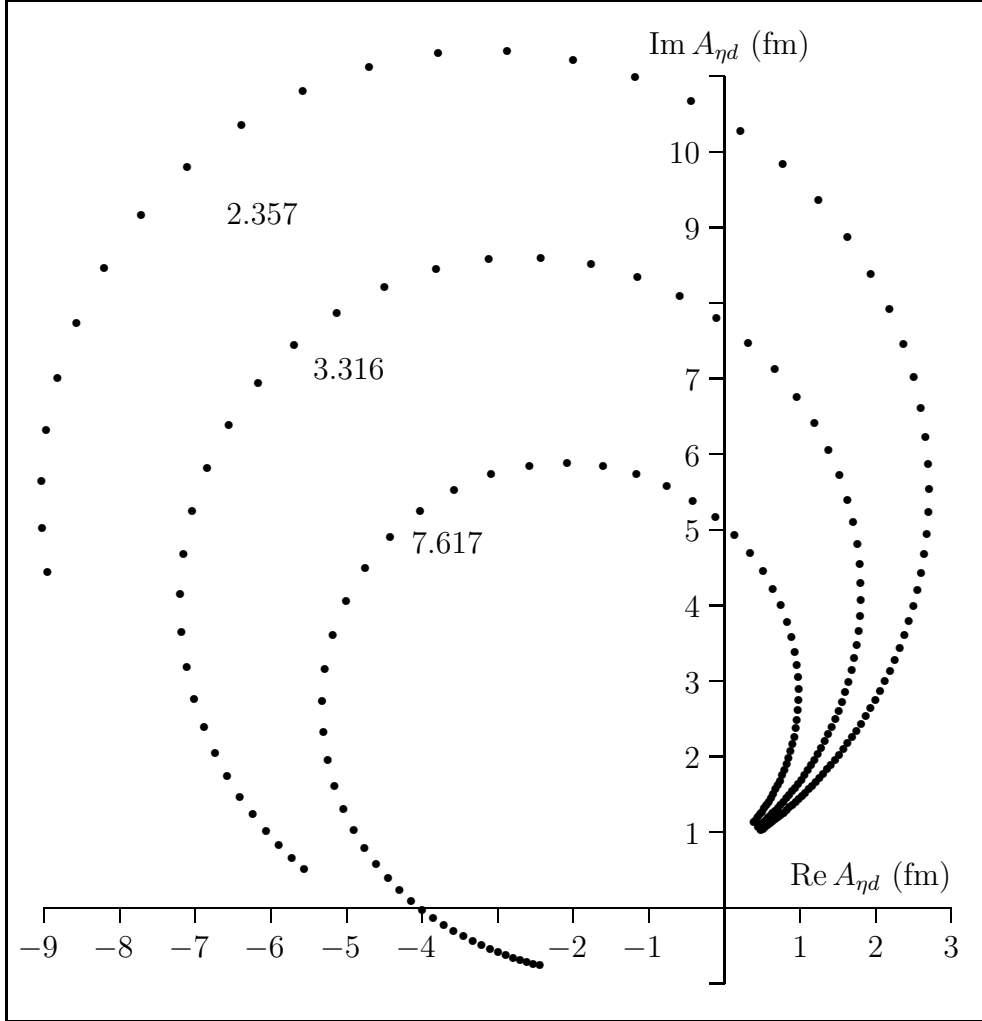


FIG. 1. The values of  $A_{\eta d}$  calculated for  $\text{Im } a_{\eta N} = 0.30 \text{ fm}$  while  $\text{Re } a_{\eta N}$  is changing from  $0.25 \text{ fm}$  to  $1 \text{ fm}$  with the step  $0.01 \text{ fm}$ . An increase of  $\text{Re } a_{\eta N}$  moves the points in the anti-clockwise direction along the curve trajectories which correspond to three choices of the range parameter  $\alpha$ .

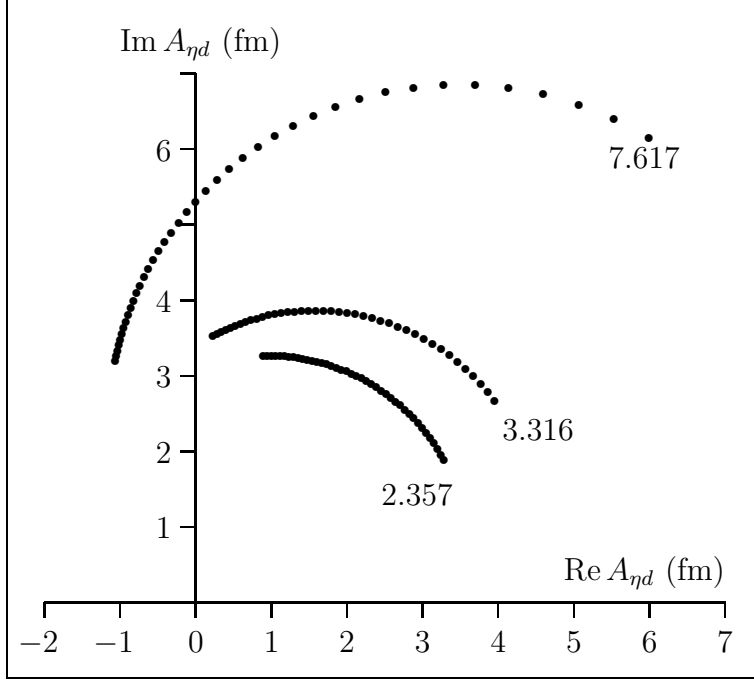


FIG. 2. The values of  $A_{\eta d}$  calculated for  $\text{Re } a_{\eta N} = 0.60$  fm while  $\text{Im } a_{\eta N}$  is changing from 0.2 fm to 0.4 fm with the step 0.005 fm. An increase of  $\text{Im } a_{\eta N}$  moves the points in the anti-clockwise direction along the curve trajectories which correspond to three choices of the range parameter  $\alpha$ .